

Metabolic Engineering of Tomato Fruit Organic Acid Content Guided by Biochemical Analysis of an Introgression Line¹[W][OA]

Megan J. Morgan, Sonia Osorio, Bernadette Gehl, Charles J. Baxter, Nicholas J. Kruger, R. George Ratcliffe, Alisdair R. Fernie, and Lee J. Sweetlove*

Department of Plant Sciences, University of Oxford, Oxford OX1 3RB, United Kingdom (M.J.M., B.G., N.J.K., R.G.R., L.J.S.); Max-Planck-Institut für Molekulare Pflanzenphysiologie, 14476 Potsdam-Golm, Germany (S.O., A.R.F.); and Syngenta, Jealott's Hill International Research Centre, Bracknell, Berkshire RG42 6EY, United Kingdom (C.J.B.)

Organic acid content is regarded as one of the most important quality traits of fresh tomato (*Solanum lycopersicum*). However, the complexity of carboxylic acid metabolism and storage means that it is difficult to predict the best way to engineer altered carboxylic acid levels. Here, we used a biochemical analysis of a tomato introgression line with increased levels of fruit citrate and malate at breaker stage to identify a metabolic engineering target that was subsequently tested in transgenic plants. Increased carboxylic acid levels in introgression line 2-5 were not accompanied by changes in the pattern of carbohydrate oxidation by pericarp discs or the catalytic capacity of tricarboxylic acid cycle enzymes measured in isolated mitochondria. However, there was a significant decrease in the maximum catalytic activity of aconitase in total tissue extracts, suggesting that a cytosolic isoform of aconitase was affected. To test the role of cytosolic aconitase in controlling fruit citrate levels, we analyzed fruit of transgenic lines expressing an antisense construct against SlAco3b, one of the two tomato genes encoding aconitase. A green fluorescent protein fusion of SlAco3b was dual targeted to cytosol and mitochondria, while the other aconitase, SlAco3a, was exclusively mitochondrial when transiently expressed in tobacco (*Nicotiana tabacum*) leaves. Both aconitase transcripts were decreased in fruit from transgenic lines, and aconitase activity was reduced by about 30% in the transgenic lines. Other measured enzymes of carboxylic acid metabolism were not significantly altered. Both citrate and malate levels were increased in ripe fruit of the transgenic plants, and as a consequence, total carboxylic acid content was increased by 50% at maturity.

Tomato (*Solanum lycopersicum*) is an important food crop of high economic value and represents a model species for fleshy fruit physiology and ripening (Giovannoni, 2004; Mueller, 2009). The breeding history of tomato has been dominated by a focus on traits that benefit the grower, such as yield, storage characteristics, and field performance (Schuch, 1994; Giovannoni, 2006; Cong et al., 2008). As a result, there has been an unintentional loss of consumer quality traits such as flavor and nutritional value, and this has focused recent interest on the molecular genetics of such traits (Giovannoni, 2001; Causse et al., 2002, 2004; Fraser et al., 2009; Mounet et al., 2009; Enfissi et al., 2010;

Centeno et al., 2011). The accumulation of a range of soluble metabolites is critically important for both flavor and nutrition. Tomato fruit undergo substantial changes in their metabolite content and composition during ripening (Carrari et al., 2006). Fruit flavor is influenced both by volatile and nonvolatile metabolites (Buttery et al., 1987; Goff and Klee, 2006; Carli et al., 2009). Of the nonvolatile metabolites, the balance between sugars and acidic compounds is of major importance for flavor (Tieman et al., 2012). The perceived flavor of tomato fruit is a complex issue, and simple associations of metabolites with flavor traits do not always hold true. Nevertheless, a network analysis of several tomato genotypes demonstrated a strong correlation between tomato fruit flavor and the main acidic metabolites: carboxylic acids, Glu, and Asp (Carli et al., 2009).

The breeding or engineering of improved flavor by increasing the amount of specific metabolites in ripe fruit requires an understanding of the biochemical and molecular factors that regulate their accumulation during the ripening process. In this study, we focused on the accumulation of citrate and malate, the most abundant of the acidic metabolites in tomato fruit. Carboxylic acids are a major component of the osmotic potential that drives cell expansion through water uptake in the expansion phase of fruit growth (Liu

¹ This work was supported by the Biotechnology and Biological Sciences Research Council and Syngenta (Collaborative Award in Science and Engineering studentship to M.J.M.), by the ERA-net Tomato Quantitative Trait Loci for Metabolites project (to S.O. and A.R.F.), and by the ERA-SysBio+ Fruit Integrative Modelling project (B.G. and L.J.S.).

* Corresponding author; e-mail lee.sweetlove@plants.ox.ac.uk.

The author responsible for distribution of materials integral to the findings presented in this article in accordance with the policy described in the Instructions for Authors (www.plantphysiol.org) is: Lee J. Sweetlove (lee.sweetlove@plants.ox.ac.uk).

[W] The online version of this article contains Web-only data.

[OA] Open Access articles can be viewed online without a subscription.

www.plantphysiol.org/cgi/doi/10.1104/pp.112.209619

et al., 2007). The concentrations of citrate and other carboxylic acids fall during this expansion phase as the cell contents are diluted (Baxter et al., 2005; Carrari et al., 2006). However, during the final stages of ripening, the level of citrate (and to a lesser extent other carboxylic acids) increases again such that it is present at high abundance in the ripe fruit. It is not known how these changes in organic acid levels are brought about. The maximal catalytic activities of enzymes of the tricarboxylic acid (TCA) cycle generally decline during fruit development, and there are no pronounced changes in activities during the later stages of ripening that correlate with the rise in organic acid levels (Steinhauser et al., 2010).

The regulation of metabolite levels is a complex issue. At the most basic level, the amount of a metabolite will change because of a difference between influx into that metabolite pool and efflux from it (Kruger and Ratcliffe, 2009). In the case of citrate, for example, one could envisage that a change in the balance of flux through the citrate synthase and aconitase reactions could be responsible for a change in citrate levels. However, the situation is complicated because citrate is synthesized in the mitochondrion but accumulates in the vacuole (Martinoia et al., 2007). Thus, the transport of citrate between these subcellular compartments will also have a bearing on its rate of accumulation (Shiratake and Martinoia, 2007). Export from the mitochondrion is by counterexchange with other carboxylic acids that are imported. Therefore, the capacity of other parts of the TCA cycle will affect the rate of export of citrate. Active uptake into the vacuole is ultimately dependent on the tonoplast membrane potential generated by the proton-pumping V-type ATPase, although citrate transport appears to occur by facilitated diffusion rather than active uptake in tomato fruit (Oleski et al., 1987). Given that TCA cycle flux is critical for the synthesis of ATP, one can see the extent to which carboxylic acid metabolism as a whole and citrate accumulation are intertwined. Accumulation in the vacuole is also a function of both the influx and efflux of citrate from the vacuole (Shimada et al., 2006) and subsequent metabolism by cytosolic isoforms of aconitase and isocitrate dehydrogenase. Given this complexity and the variety of flux modes within carboxylic acid metabolism (Sweetlove et al., 2010), it is not obvious what the best strategy for engineering increased accumulation of carboxylic acids in fleshy fruits would be. This is reflected in the range of enzymes that have been proposed to control fruit citrate accumulation, including phosphoenolpyruvate carboxylase (Guillet et al., 2002), phosphoenolpyruvate carboxykinase (Famiani et al., 2005), citrate synthase (Sadka et al., 2000a), and aconitase (Sadka et al., 2000b; Degu et al., 2011).

To identify a suitable metabolic engineering strategy for increasing carboxylic acid content of tomato, we undertook a detailed biochemical study of an introgression line of tomato (Eshed and Zamir, 1995). A specific line with an introgressed segment from

Solanum pennellii on chromosome 2 (IL2-5) was identified that showed reproducible increases in citrate and malate during the later stages of fruit development but had minimal changes in gross developmental characteristics such as fruit size and number. Although the introgressed segment contained many genes, and metabolites other than carboxylic acids were altered, we reasoned that a focused metabolic analysis would identify which of the proposed mechanisms for controlling fruit citrate accumulation was responsible for the increased citrate and malate contents in the introgression line. The effectiveness of this mechanism as a viable target for the metabolic engineering of carboxylic acid content could then be tested in transgenic plants.

RESULTS

Fruit of IL2-5 Have Increased Malate and Citrate Contents during Development

To identify a suitable line from the tomato \times *S. pennellii* introgression population (Eshed and Zamir, 1995), we grew a subset of lines that were free from major phenotypic changes (Gur et al., 2004) and measured fruit carboxylic acid content in pericarp tissue using $^1\text{H-NMR}$. We wished to identify lines in which carboxylic acids were increased at several stages of fruit development prior to the final ripe stage. This was because the biochemical changes that influence the accumulation of carboxylic acids during ripening are likely to be set prior to the final stage of maturation.

Based on our analysis, we focused on IL2-5, in which fruit citrate and malate contents were increased (Fig. 1). Fruits were analyzed at three developmental ages (30, 40, and 55 d after anthesis [DAA]). Tomatoes at 40 DAA were at breaker stage, and by 55 DAA, they were fully ripe. In comparison with the tomato 'M82' parent line, citrate was significantly increased at each of the developmental ages, with the difference between IL2-5 and cv M82 increasing during development such that ripe fruit of IL2-5 contained 60% more citrate than those of cv M82. Malate levels in IL2-5 were also significantly increased to a similar degree at 30 and 40 DAA, but in ripe fruit there was no difference compared with cv M82. Fumarate levels showed reciprocal changes to malate, with decreases in IL2-5 at 30 and 40 DAA, although the absolute amount of fumarate was a factor of 1,000 less than malate. Other carboxylic acids were not quantifiable by $^1\text{H-NMR}$ of fruit extracts. These metabolite changes were not due to an altered rate of development of IL2-5 fruit, because the main changes in carotenoid content, a key indicator of fruit developmental stage, were coincident in cv M82 and IL2-5 fruit (Supplemental Fig. S1).

To assess whether other parts of the central metabolic network were also altered in IL2-5 fruits, we determined the content of amino acids. Because amino acid synthesis draws on precursors from a number of

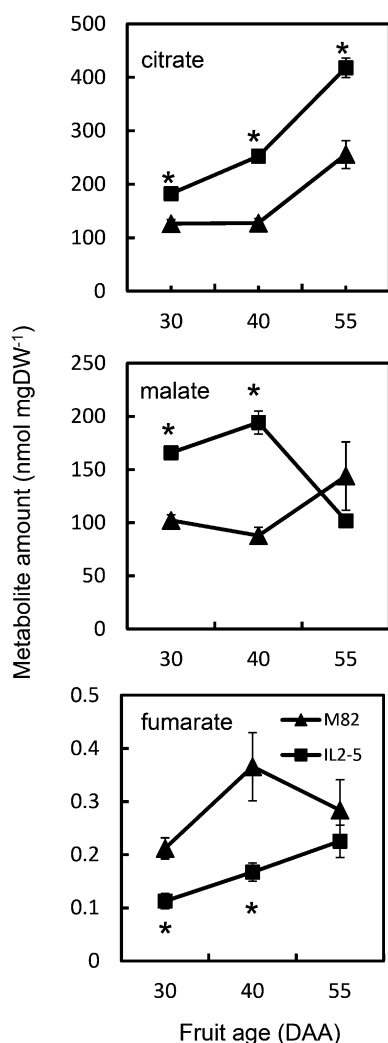


Figure 1. Carboxylic acid content of fruit of cv M82 and IL2-5 during fruit development. Organic acid content was determined by ¹H-NMR for cv M82 (triangles) and IL2-5 (squares) in extracts of pericarp tissue at 30, 40, and 55 DAA. Each value is the mean \pm SE ($n = 6$). *Values significantly different from cv M82 (Student's t test, $P < 0.05$). DW, Dry weight.

different sectors of central metabolism, they are a useful indicator of the state of the central metabolic network. As one might expect given the number of potential genetic changes due to chromosomal introgression, changes in a range of amino acids were observed (Fig. 2). Of the 19 measured amino acids, 10 were significantly increased in IL2-5 fruit. Several of these (Glu, Thr, and Met) are either directly connected to carboxylic acid metabolism or draw on carboxylic acid metabolism as a source of carbon skeletons for their biosynthesis. However, in addition, there were also increases in amino acids that are synthesized from precursors from glycolysis (Ala, Ser, Gly, Val, Leu, and Ile) and the oxidative pentose phosphate pathway (Phe).

Carbohydrate Oxidation Fluxes in IL2-5 Fruit

To assess whether the increases in citrate and malate were accompanied by major changes in flux through the central network of carbon metabolism, we incubated discs cut from the pericarp of IL2-5 and cv M82 fruit at 40 DAA (at which stage the amounts of both citrate and malate were significantly greater in IL2-5) with positionally labeled [¹⁴C]Glc. Evolved ¹⁴CO₂ was quantified at intervals over a 24-h period. The ratios of ¹⁴CO₂ released from differently labeled Glc molecules reveal information about the relative rates of different routes of carbohydrate oxidation (ap Rees, 1980). The total amount of [¹⁴C]Glc metabolized by cv M82 and IL2-5 discs was not significantly different, suggesting that the capacity for uptake of Glc and overall metabolic rate were similar between the two lines. The rate of oxidation of [¹⁴C]Glc to ¹⁴CO₂ was linear between 2 and 12 h for each positionally labeled Glc (except for [2-¹⁴C]Glc, which was only linear for the first 5 h) for both cv M82 and IL2-5 pericarp discs, suggesting that a metabolic steady state was achieved (Supplemental Fig. S2). There were no significant differences in the relative rates of oxidation of any of the differently labeled positions of Glc between IL2-5 and cv M82 (Fig. 3), suggesting that there were no substantial changes in flux through the pathways of central metabolism. Of particular relevance is the release of label from the C3,4 and C2 positions of Glc, which occurs predominantly via the TCA cycle. The release of CO₂ from C3,4 Glc relative to other carbon positions was the same in both tomato lines (Fig. 3, A–C). Similarly, the ratios of CO₂ release from C2:C1 and C1:C6 were not significantly different between lines (Fig. 3, D and E). These results indicate that the flux through the oxidative steps of the TCA cycle relative to other major carbon oxidation pathways such as the oxidative pentose phosphate pathway is unchanged in pericarp discs of the IL2-5 line.

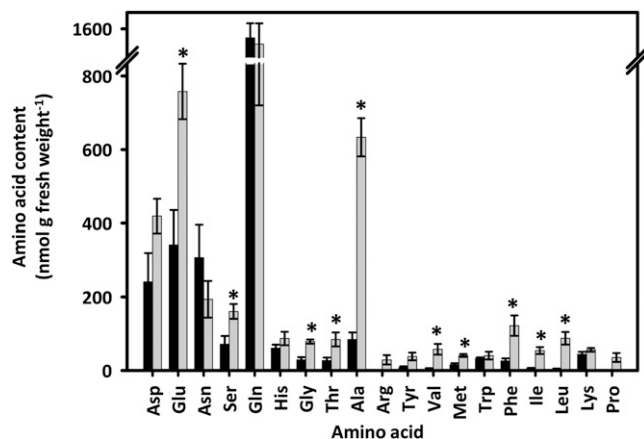
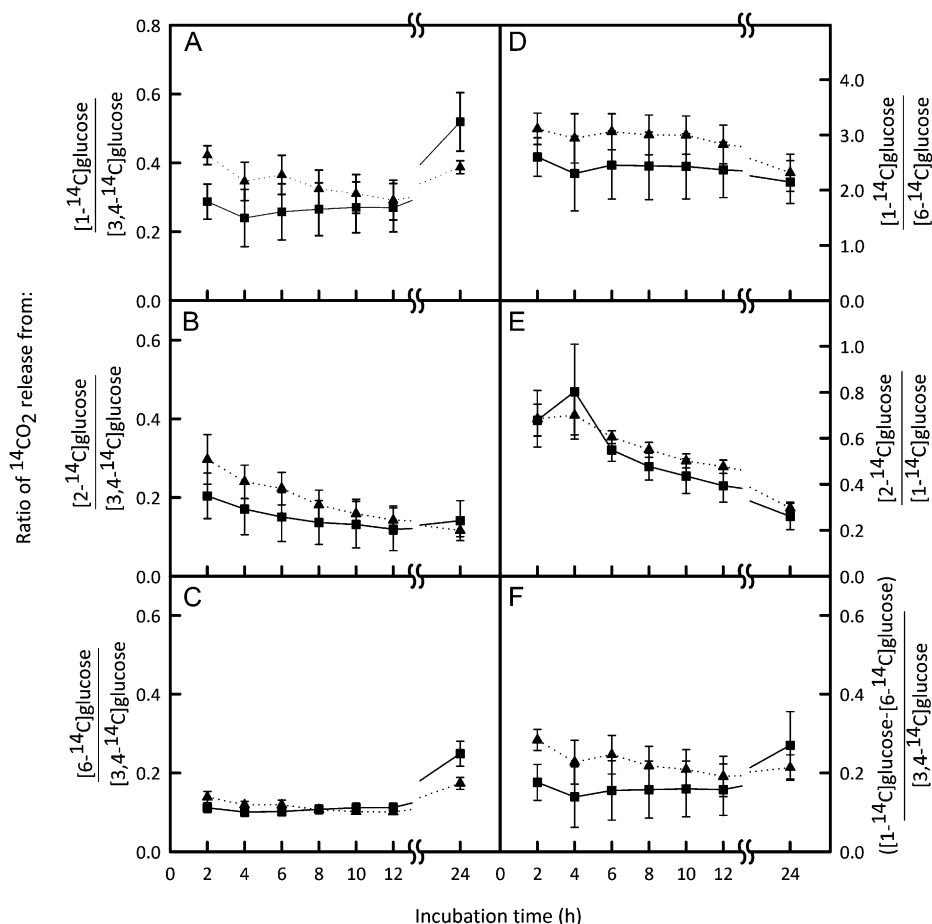


Figure 2. Amino acid contents of tomato fruit (55 DAA) from cv M82 and IL2-5. Black bars, cv M82; gray bars IL2-5. Values are means \pm SE ($n = 4$). * $P \leq 0.05$ (Student's t test).

Figure 3. Relative rates of oxidation of specific labeled Glc carbons in tomato fruit from cv M82 and IL2-5. Pericarp discs from fruit harvested 40 DAA were incubated with [1-¹⁴C]Glc, [2-¹⁴C]Glc, [3,4-¹⁴C]Glc, or [6-¹⁴C]Glc (1 mM). The ¹⁴CO₂ released by metabolism was monitored at intervals throughout a 24-h incubation period and quantified by liquid scintillation counting. Ratios of cumulative ¹⁴CO₂ release from different combinations of positionally labeled Glc for IL2-5 (squares, solid lines) and cv M82 (triangles, dotted lines) are presented. Data are ratios of the mean ± SE (n = 4). There were no significant differences (repeated-measures ANOVA) in the ratios of ¹⁴CO₂ released by cv M82 and IL2-5 for any of the combinations of positionally labeled substrates analyzed (*F* < 3.78; degrees of freedom = 1.6; *P* > 0.10).



Maximum Catalytic Activities of Enzymes of Carboxylic Acid Metabolism

The labeling experiments give a broad overview of the fluxes in central carbohydrate metabolism, but the complexity of the carbohydrate oxidation network means that it is impossible to ascribe the oxidation of a specifically labeled carbon atom exclusively to a single metabolic pathway. Moreover, the approach cannot account for complementary changes in flux through parallel pathways in different subcellular compartments. To address this latter issue, we measured the maximum catalytic activity of enzymes of carboxylic acid metabolism, both in isolated mitochondria and in crude tissue extracts, to assess the partitioning of metabolic capacity between mitochondria and other subcellular compartments. Mitochondria were isolated from 40-DAA fruit from IL2-5 and cv M82 plants, and the mitochondrial activities of seven of the eight enzymes of the TCA cycle were measured. There were no significant differences in the activities of these enzymes in IL2-5 mitochondria compared with cv M82 (Fig. 4A). We also assessed the total cellular activities of detectable enzymes of carboxylic acid metabolism in cases where there are known to be extramitochondrial isoforms (Fig. 4B). Total aconitase activity was

significantly lower in IL2-5 fruit (about one-third of the activity in cv M82 fruit). The other four enzymes measured were not significantly changed. Given that aconitase activity in isolated mitochondria was the same in the two lines, this result indicates that the cytosolic isoform of aconitase is present at substantially lower levels in IL2-5 relative to cv M82.

Metabolic Engineering of Carboxylic Acid Content of Tomato Fruit

Aconitase catalyzes the conversion of citrate to isocitrate, and it follows that a reduction in the activity of aconitase could lead to an accumulation of citrate. To examine if the reduction of total aconitase activity is brought about at the transcriptional level, and therefore would be a good target for genetic engineering, we assessed aconitase transcript levels using semi-quantitative reverse transcription (RT)-PCR. The tomato genome contains two genes encoding aconitase (Kamenetzky et al., 2010), Solyc07g052340 and Solyc12g005860. The two genes show a high degree of similarity (the predicted complementary DNA [cDNA] sequences are 88% identical), and both are most similar to ACONITASE3 (ACO3) in *Arabidopsis thaliana*;

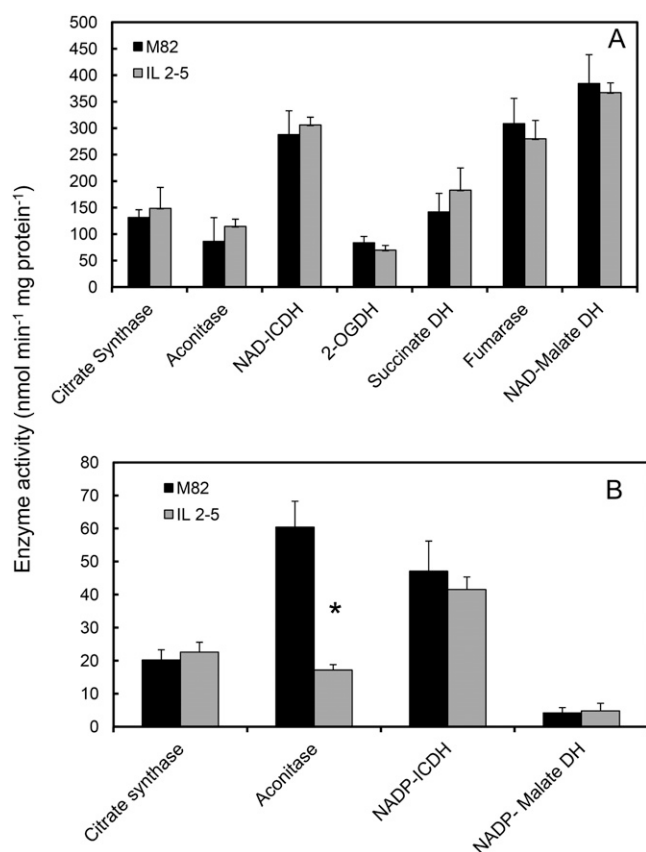


Figure 4. Maximum catalytic activities of enzymes of carboxylic acid metabolism in fruit from cv M82 and IL2-5. Enzyme activities are shown for isolated mitochondria (A) and crude pericarp extracts (B) from 40-DAA fruit. Data are means \pm se ($n = 3$). For clarity, the NAD-malate dehydrogenase activity is divided by 10. *Significantly different from cv M82 (Student's t test, $P < 0.05$). DH, Dehydrogenase; ICDH, isocitrate dehydrogenase; 2-OGDH, 2-oxoglutarate dehydrogenase. Coenzyme specificity is indicated where relevant.

Bernard et al., 2009). Accordingly, we refer to them as SlAco3a and SlAco3b, respectively. The RT-PCR results suggest that the SlAco3a transcript was slightly reduced in IL2-5 fruit (at 40 DAA) in comparison with cv M82 (Fig. 5). SlAco3b showed a less consistent pattern, with an apparent decrease in abundance in some IL2-5 samples but not others (Fig. 5).

To aid in the choice of which Aco gene to target for metabolic engineering, it would be helpful to know the subcellular localization of the respective gene products. In *Arabidopsis*, there are three aconitase genes: ACO1 encodes a cytosolic isoform, while the products of ACO2 and ACO3 are located in mitochondria (Bernard et al., 2009). The *aco-1* mutant allele in *S. pennellii* (which corresponds to SlAco3b) is deficient in both cytosolic and mitochondrial aconitase protein, suggesting that in tomato this gene product is dual targeted (Carrari et al., 2003). To investigate the subcellular targeting of both tomato Aco proteins, the SlAco genes were transiently expressed as C-terminal

GFP fusions in tobacco (*Nicotiana tabacum*) leaves (Fig. 6). The two gene products showed clear differences in subcellular localization. SlAco3a colocalized closely with mitochondria-targeted mCherry, indicating an exclusively mitochondrial localization. In contrast, SlAco3b has a more complex distribution, appearing throughout the cytosol, but it was also present in punctate bodies colocalizing with mitochondria-targeted mCherry. This suggests that SlAco3b is dual targeted to both cytosol and mitochondria and is consistent with the decrease in both cytosolic and mitochondrial aconitase in the *aco-1* mutant.

The changes in Aco transcripts suggest that Aco genes would be good targets for the engineering of altered carboxylic acid levels in tomato fruit and that to replicate the decrease in cytosolic aconitase activity in IL2-5, SlAco3b should be repressed. Therefore, we characterized fruit enzyme and metabolite levels in transgenic plants expressing an 800-bp antisense fragment of SlAco3b (van der Merwe et al., 2010). These transgenic plants were originally generated as part of a study of the role of the TCA cycle in root metabolism (van der Merwe et al., 2010), and their fruit have not been previously characterized.

Two of the transgenic lines (ACO-19 and ACO-38) were grown and allowed to set fruit. Fruit growth, size, and number in each transgenic line were indistinguishable from the wild type. Tomatoes were harvested at breaker (40 DAA) and ripe (55 DAA) stages and extracted for transcript, enzyme, and metabolite determinations. Unsurprisingly, given the high degree of sequence similarity between the two SlAco genes, both SlAco3a and SlAco3b transcripts were significantly decreased in the two transgenic lines in fruit at both 40 and 55 DAA (Fig. 7). The exception was line ACO19, in which SlAco3b was significantly altered in 40-DAA fruit but not in fruit from the later developmental time point. However, aconitase activity was decreased by about 30% compared with the wild type in both lines at both stages of fruit development (Table I). Although the activity of aconitase increased developmentally in wild-type and transgenic lines between the 40- and 55-DAA stages, the relative decrease in activity in the transgenic lines was maintained at around 30%. None of the other measured enzymes of carboxylic acid metabolism were significantly different

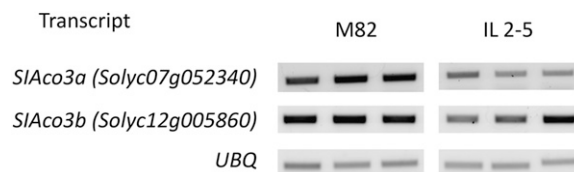
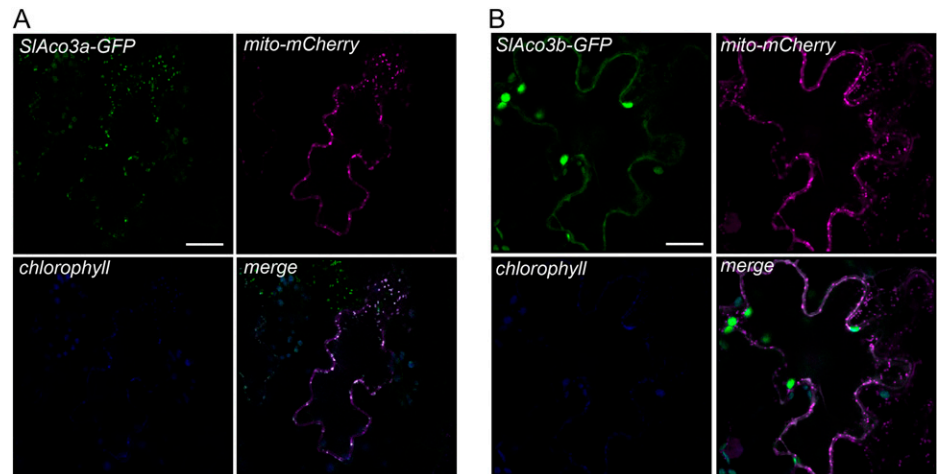


Figure 5. Semiquantitative RT-PCR analysis of aconitase transcript abundance in cv M82 and IL2-5 fruit at 40 DAA. Replicate PCR products were amplified from cDNA template prepared from three independent fruit of cv M82 and IL2-5 plants. The transcript encoding ubiquitin (UBQ) was used as a control.

Figure 6. Subcellular localization of SlAco3a and SlAco3b. Gene constructs consisting of SlAco genes fused C-terminally to GFP and driven by the Arabidopsis UBIQUITIN10 promoter were transiently expressed in tobacco leaves by agroinfiltration. GFP fluorescence was colocalized with mitochondrially targeted mCherry (mito-mCherry). GFP fluorescence of SlAco3a-GFP (A) and SlAco3b-GFP (B) with mito-mCherry signal is indicated. Chlorophyll autofluorescence is also shown. Bars = 20 μm .



in the transgenic fruit compared with the wild type at either stage of development (Table I).

To establish whether the transgenic manipulation had the predicted effect on citrate levels, fruit carboxylic acids were quantified by gas chromatography-mass spectrometry (GC-MS; Table II). In ripe fruit, citrate was significantly increased in both transgenic lines by about 40%, confirming successful metabolic engineering. In contrast to the introgression line, however, this increase in citrate was not apparent at the earlier developmental stage (40 DAA) in the transgenic fruit. The increases in citrate in ripe fruit were roughly proportional to the decrease in aconitase levels in both the introgression and transgenic lines. In IL2-5, total aconitase activity decreased by 66% and citrate increased by 60%. In the transgenic lines, aconitase decreased by approximately 30% and citrate increased by 40%.

In the transgenic fruit, other carboxylic acids were also significantly altered compared with the wild type in ripe fruit but, as with citrate, not at the early 40-DAA stage. Malate increased and fumarate and succinate decreased (Table II). These changes were similar to those seen in the introgression line at 40 DAA. However, the changes in malate and fumarate in the introgression lines were not apparent in ripe fruit, indicating that the developmental timing of the perturbation of this sector of carboxylic acid metabolism is different in the transgenic lines. The fact that the transgenic lines were not an exact biochemical phenocopy of the introgression lines is to be expected, given the presence of many other background genetic changes in the introgression lines and differences in the timing and extent of change of aconitase activity in the transgenic lines. Nevertheless, in quantitative terms, the changes in fumarate and malate were proportional to the decrease in aconitase activity in both the introgression and transgenic lines. Fumarate decreased proportionately to aconitase: fumarate decreased by 54% in the introgression line and an average of 37% in the transgenic lines (approximately matching the 66% and 30% decreases of aconitase,

respectively). Malate increased by 120% in the introgression fruit and an average of 76% in the transgenic fruit, meaning an increase of roughly twice the decrease in aconitase activity. Total carboxylic acid (malate + citrate + succinate + fumarate) increased from an average of 99 $\mu\text{g g}^{-1}$ fresh weight in wild-type

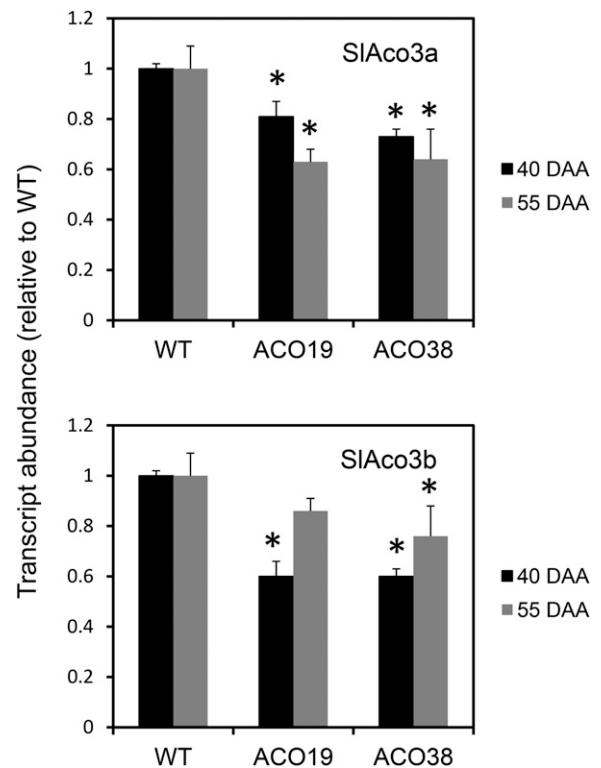


Figure 7. Abundance of SlAco3a and SlAco3b transcripts in fruit from antisense transgenic lines. RNA was extracted from fruit from the wild type (WT) and transgenic lines (ACO22 and ACO38) at 40 and 55 DAA. SlAco3a and SlAco3b transcripts were quantified by quantitative real-time PCR. Mean abundance values (relative to the wild type) \pm SE of three biological replicates are shown. *Significantly different from the wild type (Student's *t* test, $P < 0.05$).

Table I. Maximum catalytic activities of enzymes of carboxylic acid metabolism in fruit of wild-type and transgenic tomato plants expressing an antisense aconitase construct

Tomatoes harvested at 40 and 55 DAA were extracted, and the maximal catalytic activities of six enzymes of carboxylic acid metabolism were measured. The wild type and two independent transgenic lines (ACO19 and ACO38) were assessed. Each value is the mean \pm SE of six biological replicates. Values significantly different from the wild type are indicated in boldface (Student's *t* test, $P < 0.05$).

Enzyme	Enzyme Activity					
	40 DAA			55 DAA		
	Wild Type	ACO19	ACO38	Wild Type	ACO19	ACO38
	<i>nmol min⁻¹ g⁻¹ fresh wt</i>					
Aconitase	20.1 \pm 5.3	13.1 \pm 3.4	12.5 \pm 3.9	32.5 \pm 4.8	24.7 \pm 3.9	22.6 \pm 6.1
Succinate dehydrogenase	0.73 \pm 0.12	0.87 \pm 0.09	0.77 \pm 0.14	1.03 \pm 0.15	0.93 \pm 0.06	0.89 \pm 0.10
Fumarase	190 \pm 32.3	202 \pm 25.7	182 \pm 28.6	150 \pm 22.3	135 \pm 15.7	143 \pm 18.7
NAD ⁺ -malate dehydrogenase	3521 \pm 145	3152 \pm 188	3698 \pm 132	1024 \pm 89	896 \pm 110	963 \pm 138
Citrate synthase	11.3 \pm 1.8	10.8 \pm 1.5	9.7 \pm 1.5	5.3 \pm 1.7	4.3 \pm 1.9	5.8 \pm 1.9
NADP-isocitrate dehydrogenase	22.5 \pm 2.5	20.8 \pm 3.6	18.9 \pm 4.4	60.5 \pm 5.8	62.5 \pm 7.7	55.5 \pm 6.9

fruit to 140 and 157 $\mu\text{g g}^{-1}$ fresh weight in ACO-19 and ACO-22 fruit, respectively.

DISCUSSION

Decreased Activity of Cytosolic Aconitase Correlates with Altered Carboxylic Acid Content in Fruit of an Introgression Line

Fruit of the selected introgression line, IL2-5, contained elevated levels of citrate and malate and a decrease in fumarate at breaker stage relative to the cv M82 parent line. The increase in citrate persisted until ripeness under our growth conditions, although this trait may not be stable under all conditions because no increase in citrate was recorded in the ripe fruit of this introgression line when grown in the field (Schauer et al., 2006, 2008). We found no evidence of major changes in fluxes through relevant metabolic pathways in the IL2-5 fruit, reflecting the nonintuitive relationship between metabolite levels and flux (Williams et al., 2008; Kruger and Ratcliffe, 2009).

There was, however, a significant decrease in the maximum catalytic activity of one of the enzymes of carboxylic acid metabolism: aconitase. This change in activity was not apparent in isolated mitochondria, suggesting that it was a cytosolic isoform of aconitase that was altered. Analysis of transiently expressed GFP fusions of the two tomato aconitases in tobacco leaves

showed that while SlAco3a is localized exclusively in mitochondria, SlAco3b appears to be dual targeted to both mitochondria and cytosol. There is a precedent for this in yeast, in which aconitase is thought to be dual targeted by inefficient import into mitochondria or by release of the mitochondrially imported enzyme back into the cytosol (Regev-Rudzki et al., 2005).

The relationship between aconitase activity and genotype in the introgression line is not direct, because the two aconitase genes lie on chromosomes 7 and 12 and therefore are not within the introgressed segment on chromosome 2. RT-PCR suggests a slight decrease in expression of the two SlAco genes, so perhaps the introgressed region in IL2-5 contains a transcriptional regulator of the aconitase gene. This possibility is supported by the identification of several enzyme quantitative trait loci in the same introgression line population in which the introgressed region does not contain the structural gene of the enzyme concerned (Steinhauser et al., 2011).

Aconitase Activity Is a Determinant of Fruit Citrate Levels

A decrease in the activity of aconitase provides an obvious link to the accumulation of citrate, its substrate. Perturbation of the TCA cycle could also provide an explanation for changes in other carboxylic acids. Further evidence that the change in citrate is directly linked to aconitase activity and not some other

Table II. Carboxylic acid content of fruit of transgenic plants expressing an antisense aconitase construct

Fruit extracts were analyzed using GC-MS. Tomatoes were harvested at 40 and 55 DAA as indicated. Data are means \pm SE of six independent fruits. Values in boldface are significantly different from the wild type (Student's *t* test, $P < 0.05$).

Metabolite	Metabolite Level in Fruit (Relative to the Wild Type)					
	40 DAA			55 DAA		
	Wild Type	ACO19	ACO38	Wild Type	ACO19	ACO38
Citrate	1.00 \pm 0.04	0.84 \pm 0.06	0.70 \pm 0.08	1.00 \pm 0.03	1.38 \pm 0.05	1.42 \pm 0.05
Succinate	1.00 \pm 0.02	1.12 \pm 0.02	1.17 \pm 0.03	1.00 \pm 0.02	0.81 \pm 0.00	0.80 \pm 0.00
Fumarate	1.00 \pm 0.08	1.21 \pm 0.07	1.01 \pm 0.02	1.00 \pm 0.03	0.62 \pm 0.02	0.64 \pm 0.02
Malate	1.00 \pm 0.08	0.79 \pm 0.04	0.98 \pm 0.10	1.00 \pm 0.10	1.63 \pm 0.24	1.89 \pm 0.14

background effect in the introgression line was provided by direct manipulation of aconitase activity in transgenic plants. In fact, the increase in citrate in ripe fruit was quantitatively proportional to the decrease in aconitase in both the introgression and transgenic lines, suggesting that aconitase activity is a major determinant of ripe fruit citrate levels. In support of this, pharmacological inhibition of aconitase in lemon (*Citrus limon*) fruit also led to an increase in citrate levels (Degu et al., 2011). Aconitase activity is also linked to citrate levels in other tissues in tomato: leaf citrate levels were also increased in the *aco-1* mutant (Carrari et al., 2003). However, it is worth noting that, in the transgenic lines, the decreased aconitase activity at the earlier fruit developmental stage (40 DAA) did not result in a significant increase in citrate level. This suggests that other factors, in addition to aconitase activity, influence fruit citrate level. The difference in the relationship between aconitase and citrate at this developmental stage in transgenic versus introgression line fruit is most likely due to the difference in background genotype (cv Moneymaker versus cv M82, respectively).

Citrate synthase might also be expected to influence citrate levels, and this was demonstrated in the leaves of transgenic tomato plants with reduced citrate synthase (Sienkiewicz-Porzucek et al., 2008). However, there was no direct relationship between citrate synthase activity and citrate levels in arsenite-treated citrus (Sadka et al., 2000a). Transgenic manipulation to decrease the activity of NAD-isocitrate dehydrogenase, the enzyme immediately downstream of aconitase, had no effect on tomato leaf citrate levels (Sienkiewicz-Porzucek et al., 2010). It appears that there is not a simple relationship between carboxylic acid levels and the activity of the enzymes that catalyze their interconversion (Nunes-Nesi et al., 2008). This disconnect between the metabolite levels and maximum catalytic activities of enzymes extends throughout the network of central carbon metabolism (Sulpice et al., 2010); therefore, the effect of altered aconitase activity on citrate levels may be considered somewhat exceptional.

Aconitase Activity Also Affects the Accumulation of Other Carboxylic Acids

In addition to increasing citrate content in ripe fruit, transgenic suppression of aconitase also led to a substantial increase in malate as well as decreases in succinate and fumarate. Perturbation of several carboxylic acids by manipulation of a single TCA cycle enzyme is not uncommon (Araújo et al., 2012) and is a reflection of the interconnected nature of carboxylic acid metabolism. Similar changes in carboxylic acid levels were seen in the introgression line, where the change in aconitase activity was restricted to the cytosol.

Interpretation of these changes is complicated by the compartmentation of TCA metabolism and may not be directly related to mitochondrial carboxylic acid metabolism. For instance, the levels of predominantly

vacuolar carboxylic acids such as citrate and malate are influenced by the rate of export of these metabolites from mitochondria. In heterotrophic *Arabidopsis* cells, these export fluxes are 1 order of magnitude lower than the mitochondrial TCA cycle fluxes (Williams et al., 2008). Thus, changes in the accumulation rate of citrate and malate can be caused by proportionally small changes in mitochondrial TCA cycle flux that may be within the error range of the flux estimate (and therefore undetectable). This most likely explains the lack of detectable change of overall carboxylic acid oxidation in the introgression line fruit and further suggests that flux through the cytosolic pathway of citrate metabolism is low in relation to the mitochondrial pathway. Alternatively, there could be a compensatory increase in flux through the mitochondrial pathway (Morgan et al., 2008).

The opposing changes in fumarate and malate may also be explained by the compartmentation of these metabolites. In mitochondria, the interconversion of fumarate and malate is close to equilibrium, so one would expect the levels of these two metabolites to follow one another. The observed decreased fumarate and increased malate levels in both the transgenic and introgression line fruit reflects the fact that the measured malate is mainly extramitochondrial (vacuolar). Most likely, an increased efflux of malate from the mitochondrion leads to increased accumulation of malate in the vacuole. Malate concentration in the mitochondrion is probably decreased, in line with the decreased fumarate content.

The function of cytosolic aconitase in ripening fruit is unclear. One suggestion is that it is involved in the metabolism of citrate released from the vacuole to provide an entry point into amino acid metabolism or the γ -aminobutyrate shunt in lemon (Degu et al., 2011). However, in tomato fruit, citrate is accumulating at the phase of ripening under consideration, so extensive efflux of citrate from the vacuole seems unlikely. An alternative possibility is that the metabolism of citrate in the cytosol contributes to cytosolic NADPH provision by providing a substrate for the NADP-dependent isocitrate dehydrogenase or is important for the generation of carbon skeletons for the synthesis of Glu and Asp, both of which accumulate substantially in the later phases of tomato ripening (Baxter et al., 2005).

CONCLUSION

This study demonstrates that individual lines of genetic mapping populations can provide useful information to guide metabolic engineering strategies. Although such lines contain relatively large regions of introgressed DNA from a genetically distinct parental line, detailed biochemical analysis can pinpoint the main point of metabolic disturbance and highlight potential candidate proteins that can be tested in a targeted manner in transgenic plants. Here, the introgression line

allowed us to focus specifically on aconitase among myriad possible targets for manipulation of the accumulation of carboxylic acids in tomato fruit. One could envisage further refinement of the transgenic manipulation by using fruit-specific promoters that are more finely tuned to the appropriate developmental stage and take into account the variations in metabolism within different fruit tissues (Moco et al., 2007; Matas et al., 2011).

MATERIALS AND METHODS

Plant Material

Seeds of tomato (*Solanum lycopersicum* 'M82') and introgression line 2-5 (incorporating a segment from *Solanum pennellii*) were kindly supplied by the Tomato Genetics Resource Centre. Transgenic tomato 'Moneymaker' expressing an antisense aconitase construct were described previously (van der Merwe et al., 2010). Plants were grown in a 16-h photoperiod at 22°C to 23°C day temperature/20°C to 22°C night temperature and with supplementary lighting to maintain an irradiance of 250 to 400 $\mu\text{mol m}^{-2} \text{s}^{-1}$. Plants were grown in a standard potting compost supplemented with slow-release fertilizer. Tomato feed was applied during flowering and fruit set, and a 0.5% (w/v) calcium chloride solution was sprayed directly onto all developing fruit weekly to help control blossom end rot.

Analysis of Carboxylic Acids by $^1\text{H-NMR}$

Freeze-dried pericarp tissue was extracted in 70% tetradeuteromethanol/30% deuterated water exactly as described (Le Gall et al., 2003). $^1\text{H-NMR}$ spectra were recorded at 20°C on a Varian Unity Inova 600 spectrometer using a 5-mm HCN triple resonance z-gradient probe and the standard Varian pulse sequence with a relaxation delay of 2 s, including a presaturation pulse to suppress the residual water signal, a 90° pulse angle, a spectral width of 10 ppm, and a 4-s acquisition time. Tetradeuteromethanol was used for the internal lock signal, and 320 transients were collected for each spectrum. Spectra were processed and analyzed using NUTS (Acorn NMR). A 1-Hz line broadening was applied before Fourier transformation, and peaks were integrated manually within NUTS.

Analysis of Carboxylic Acids by GC-MS

Frozen pericarp tissue powder was extracted in chloroform-methanol, and carboxylic acids were quantified by GC-MS as described previously (Roessner et al., 2001), following a procedure optimized for tomato tissue (Roessner-Tunali et al., 2003).

Analysis of Amino Acid Content

Frozen pericarp tissue powder was extracted in 0.1 M HCl, and proteinogenic amino acids were quantified by HPLC (Bruckner et al., 1995).

Carbohydrate Oxidation Fluxes

Freshly harvested pericarp discs (10 mm diameter, 3 mm thick) were washed in 10 mM MES-KOH (pH 6.5). Eight discs were placed into 100-mL flasks containing 5.0 mL of 10 mM MES-KOH (pH 6.5) with 1 mM Glc supplemented with [1- ^{14}C]Glc, [2- ^{14}C]Glc, [3,4- ^{14}C]Glc, or [6- ^{14}C]Glc (3.7 kBq per flask). Evolved $^{14}\text{CO}_2$ was trapped in 0.5 mL of 10% (w/v) KOH and radioactivity quantified by liquid scintillation counting (Harrison and Kruger, 2008).

Isolation of Mitochondria

Fresh tomato pericarp tissue was roughly chopped, and 50 to 100 g was placed in a square-section polycarbonate container with 200 to 300 mL of extraction medium (0.3 M Suc, 25 mM tetrasodium pyrophosphate, 25 mM TES-KOH [pH 7.5], 2 mM EDTA, 10 mM KH_2PO_4 , 1% [w/v] polyvinylpyrrolidone-40, 1% [w/v] bovine serum albumin, and 20 mM ascorbic acid). The sample

was homogenized using multiple short bursts (less than 1 s) of a Status Polytron blender (Kinematica) on a low setting (4). The sample was filtered through one layer of Miracloth and two layers of muslin. The filtrate was centrifuged at 1,085g for 5 min. The pellet was discarded, and the supernatant was centrifuged for 15 min at 23,500g. The pellet was resuspended in wash buffer (0.3 M Suc, 10 mM TES-KOH [pH 7.2], and 0.1% [w/v] bovine serum albumin) to an approximate final volume of 2 mL before being layered onto a 35-mL gradient of 0% to 4.4% (w/v) polyvinylpyrrolidone-40 in 18% (v/v) Percoll. The gradient was centrifuged at 40,000g for 40 min, and the mitochondria were removed from the band near the bottom of the gradient using a 5-mL pipette. The mitochondria were diluted with wash buffer and centrifuged twice at 27,000g for 15 min. The final pellet was resuspended in a minimal volume of wash buffer.

Enzyme Assays

Maximum catalytic activities of the enzymes of carboxylic acid metabolism were measured spectrophotometrically in desalted extracts of pericarp tissue or in isolated mitochondria according to Morgan et al. (2008).

Semiquantitative RT-PCR

The following primers were used to amplify *Solyc07g052340* (forward, 5'-CATGAACAACCTTGGCAGTG-3'; reverse, 5'-GCAGCTTCTGCCTCAATACC-3') and *Solyc12g005860* (forward, 5'-TCCACAAAGATAGCCCTGCT-3'; reverse, 5'-TCCCATTCTACCAAGTTGC-3') from fruit pericarp cDNA. Cycle numbers and annealing temperatures were optimized for each template to ensure that the amplification reaction was tested in the exponential phase. Products were visualized using ethidium bromide after separation by agarose gel electrophoresis.

Quantitative Real-Time PCR

The following primers were used to amplify *Solyc07g052340* (forward, 5'-GCCGCTTGCTTCAACTTCTAC-3'; reverse, 5'-GACTCCACCTCGGCACAGA-3') and *Solyc12g005860* (forward, 5'-TGGTGCTTATTGCTCTAGTGGGTA-3'; reverse, 5'-CAACACCGTATCTCCACCTCA-3'). cDNA amplification was quantified using the fluorescent intercalating dye SYBR Green in an iCycler detection system (Bio-Rad). Transcript abundance was normalized against UBQUITIN3 and amplified using the following primers (forward, 5'-AGGTGATGACACTGGAAAGGT-3'; reverse, 5'-ATCGCCTCCAGCCTTGTGTA-3').

Subcellular Localization of SIACO-GFP Fusion Proteins Transiently Expressed in Tobacco Leaves

SIACO3a and *SIACO3b* were PCR amplified from fruit cDNA using the following primer pairs: *SIACO3a_for* (5'-caccATGTATAGTAATACAGCTCGCAAGTAC-3') and *SIACO3a_rev* (5'-TTGCTTTGTCAATTGACGAATGACATATTG-3'); *SIACO3b_for* (5'-caccATGTACGTTTCTTCTTCTGTTACATCAAAAC-3') and *SIACO3b_rev* (5'-TTGCTGACTCAACTGTGCAATGACGTATG-3'). Purified PCR products were subcloned into pUBI10-GFP (Grefen et al., 2010) and transformed into *Agrobacterium tumefaciens* strain GV3101. Transformed agrobacteria were infiltrated into mature tobacco (*Nicotiana tabacum*) leaves together with *A. tumefaciens* containing expression constructs for mitochondria-targeted mCherry (Nelson et al., 2007). Four days after infiltration, excised leaf tissue was imaged on a Leica DM6000 CS confocal microscope (Leica Microsystems). GFP was excited with an argon 488 laser at 35% power, and GFP signal was collected between 505 and 525 nm. The mCherry fluorophore was excited with the HeNe 534-nm laser set to 25% power, and emitted signal was collected between 595 and 620 nm. Chlorophyll fluorescence was collected with HeNe 543-nm excitation at 20% power between 650 and 720 nm. Images were processed using Leica LAS AF Lite software.

Statistical Analyses

Student's *t* test (two tailed, unequal variance) was used to determine the significance of differences in enzyme activities and metabolite levels between tomato lines. The mean \pm SE of ratios of $^{14}\text{CO}_2$ release from positionally labeled Glc were subjected to log transformation prior to repeated-measures

ANOVA based on type III sums of squares (SPSS/PASW Statistics 18; IBM). The homogeneity of variance of the dependent variable in repeated-measures ANOVA was confirmed using Levene's test prior to assessing the significance of differences between plant lines. Only statistical differences for which $P < 0.05$ were considered significant.

Supplemental Data

The following materials are available in the online version of this article.

Supplemental Figure S1. Carotenoid content of cv M82 and IL2-5 fruit during development.

Supplemental Figure S2. Rate of oxidation of [^{14}C]Glc to $^{14}\text{CO}_2$ by tomato pericarp discs from cv M82 and IL2-5 fruits is linear over the first 12 h.

Received October 23, 2012; accepted November 16, 2012; published November 19, 2012.

LITERATURE CITED

- ap Rees T (1980) Assessment of the contribution of metabolic pathways to respiration. In DD Davies, ed, *The Biochemistry of Plants*, Vol 2. Academic Press, New York, pp 1–29
- Araújo WL, Nunes-Nesi A, Nikoloski Z, Sweetlove LJ, Fernie AR (2012) Metabolic control and regulation of the tricarboxylic acid cycle in photosynthetic and heterotrophic plant tissues. *Plant Cell Environ* 35: 1–21
- Baxter CJ, Carrari F, Bauke A, Overy S, Hill SA, Quick PW, Fernie AR, Sweetlove LJ (2005) Fruit carbohydrate metabolism in an introgression line of tomato with increased fruit soluble solids. *Plant Cell Physiol* 46: 425–437
- Bernard DG, Cheng Y, Zhao Y, Balk J (2009) An allelic mutant series of ATM3 reveals its key role in the biogenesis of cytosolic iron-sulfur proteins in Arabidopsis. *Plant Physiol* 151: 590–602
- Bruckner H, Langer M, Lupke M, Westhauser T, Godel H (1995) Liquid chromatographic determination of amino acid enantiomers by derivatization with o-phthalaldehyde and chiral thiols: applications with reference to food science. *J Chromatog* 697: 229–245
- Buttery RG, Teranishi R, Ling LC (1987) Fresh tomato aroma volatiles: a quantitative study. *J Agric Food Chem* 35: 540–544
- Carli P, Arima S, Fogliano V, Tardella L, Frusciante L, Ercolano MR (2009) Use of network analysis to capture key traits affecting tomato organoleptic quality. *J Exp Bot* 60: 3379–3386
- Carrari F, Baxter C, Usadel B, Urbanczyk-Wocniak E, Zanor MI, Nunes-Nesi A, Nikiforova V, Centero D, Ratzka A, Pauly M, et al (2006) Integrated analysis of metabolite and transcript levels reveals the metabolic shifts that underlie tomato fruit development and highlight regulatory aspects of metabolic network behavior. *Plant Physiol* 142: 1380–1396
- Carrari F, Nunes-Nesi A, Gibon Y, Lytovchenko A, Loureiro ME, Fernie AR (2003) Reduced expression of aconitase results in an enhanced rate of photosynthesis and marked shifts in carbon partitioning in illuminated leaves of wild species tomato. *Plant Physiol* 133: 1322–1335
- Causse M, Duffe P, Gomez MC, Buret M, Damidaux R, Zamir D, Gur A, Chevalier C, Lemaire-Chamley M, Rothan C (2004) A genetic map of candidate genes and QTLs involved in tomato fruit size and composition. *J Exp Bot* 55: 1671–1685
- Causse M, Saliba-Colombani V, Lecomte L, Duffé P, Rousselle P, Buret M (2002) QTL analysis of fruit quality in fresh market tomato: a few chromosome regions control the variation of sensory and instrumental traits. *J Exp Bot* 53: 2089–2098
- Centeno DC, Osorio S, Nunes-Nesi A, Bertolo AL, Carneiro RT, Araújo WL, Steinhäuser MC, Michalska J, Rohrmann J, Geigenberger P, et al (2011) Malate plays a crucial role in starch metabolism, ripening, and soluble solid content of tomato fruit and affects postharvest softening. *Plant Cell* 23: 162–184
- Cong B, Barrero LS, Tanksley SD (2008) Regulatory change in YABBY-like transcription factor led to evolution of extreme fruit size during tomato domestication. *Nat Genet* 40: 800–804
- Degu A, Hatew B, Nunes-Nesi A, Shlizerman L, Zur N, Katz E, Fernie AR, Blumwald E, Sadka A (2011) Inhibition of aconitase in citrus fruit callus results in a metabolic shift towards amino acid biosynthesis. *Planta* 234: 501–513
- Enfissi EM, Barneche F, Ahmed I, Lichtlé C, Gerrish C, McQuinn RP, Giovannoni JJ, Lopez-Juez E, Bowler C, Bramley PM, et al (2010) Integrative transcript and metabolite analysis of nutritionally enhanced DE-ETIOLATED1 downregulated tomato fruit. *Plant Cell* 22: 1190–1215
- Eshed Y, Zamir D (1995) An introgression line population of *Lycopersicon pennellii* in the cultivated tomato enables the identification and fine mapping of yield-associated QTL. *Genetics* 141: 1147–1162
- Famiani F, Cultrera NGM, Battistelli A, Casulli V, Proietti P, Standardi A, Chen ZH, Leegood RC, Walker RP (2005) Phosphoenolpyruvate carboxykinase and its potential role in the catabolism of organic acids in the flesh of soft fruit during ripening. *J Exp Bot* 56: 2959–2969
- Fraser PD, Enfissi EM, Bramley PM (2009) Genetic engineering of carotenoid formation in tomato fruit and the potential application of systems and synthetic biology approaches. *Arch Biochem Biophys* 483: 196–204
- Giovannoni J (2001) Molecular biology of fruit maturation and ripening. *Annu Rev Plant Physiol Plant Mol Biol* 52: 725–749
- Giovannoni JJ (2004) Genetic regulation of fruit development and ripening. *Plant Cell (Suppl)* 16: S170–S180
- Giovannoni JJ (2006) Breeding new life into plant metabolism. *Nat Biotechnol* 24: 418–419
- Goff SA, Klee HJ (2006) Plant volatile compounds: sensory cues for health and nutritional value? *Science* 311: 815–819
- Grefen C, Donald N, Hashimoto K, Kudla J, Schumacher K, Blatt MR (2010) A ubiquitin-10 promoter-based vector set for fluorescent protein tagging facilitates temporal stability and native protein distribution in transient and stable expression studies. *Plant J* 64: 355–365
- Guillet C, Just D, Bénard N, Destrac-Irvine A, Baldet P, Hernould M, Causse M, Raymond P, Rothan C (2002) A fruit-specific phosphoenolpyruvate carboxylase is related to rapid growth of tomato fruit. *Planta* 214: 717–726
- Gur A, Semel Y, Cahaner A, Zamir D (2004) Real time QTL of complex phenotypes in tomato interspecific introgression lines. *Trends Plant Sci* 9: 107–109
- Harrison PW, Kruger NJ (2008) Validation of the design of feeding experiments involving [^{14}C]substrates used to monitor metabolic flux in higher plants. *Phytochemistry* 69: 2920–2927
- Kamenetzky L, Asís R, Bassi S, de Godoy F, Bermúdez L, Fernie AR, Van Sluys MA, Vrebalov J, Giovannoni JJ, Rossi M, et al (2010) Genomic analysis of wild tomato introgressions determining metabolism- and yield-associated traits. *Plant Physiol* 152: 1772–1786
- Kruger NJ, Ratcliffe RG (2009) Insights into plant metabolic networks from steady-state metabolic flux analysis. *Biochimie* 91: 697–702
- Le Gall G, Colquhoun IJ, Davis AL, Collins GJ, Verhoeven ME (2003) Metabolite profiling of tomato (*Lycopersicon esculentum*) using ^1H NMR spectroscopy as a tool to detect potential unintended effects following a genetic modification. *J Agric Food Chem* 51: 2447–2456
- Liu HF, Génard M, Guichard S, Bertin N (2007) Model-assisted analysis of tomato fruit growth in relation to carbon and water fluxes. *J Exp Bot* 58: 3567–3580
- Martinoia E, Maeshima M, Neuhaus HE (2007) Vacuolar transporters and their essential role in plant metabolism. *J Exp Bot* 58: 83–102
- Matas AJ, Yeats TH, Buda GJ, Zheng Y, Chatterjee S, Tohge T, Ponnala L, Adato A, Aharoni A, Stark R, et al (2011) Tissue- and cell-type specific transcriptome profiling of expanding tomato fruit provides insights into metabolic and regulatory specialization and cuticle formation. *Plant Cell* 23: 3893–3910
- Moco S, Capanoglu E, Tikunov Y, Bino RJ, Boyacioglu D, Hall RD, Vervoort J, De Vos RC (2007) Tissue specialization at the metabolite level is perceived during the development of tomato fruit. *J Exp Bot* 58: 4131–4146
- Morgan MJ, Lehmann M, Schwarzländer M, Baxter CJ, Sienkiewicz-Porzucek A, Williams TC, Schauer N, Fernie AR, Fricker MD, Ratcliffe RG, et al (2008) Decrease in manganese superoxide dismutase leads to reduced root growth and affects tricarboxylic acid cycle flux and mitochondrial redox homeostasis. *Plant Physiol* 147: 101–114
- Mounet F, Moing A, Garcia V, Petit J, Maucourt M, Deborde C, Bernillon S, Le Gall G, Colquhoun I, Defernez M, et al (2009) Gene and metabolite regulatory network analysis of early developing fruit tissues highlights new candidate genes for the control of tomato fruit composition and development. *Plant Physiol* 149: 1505–1528
- Mueller LA (2009) A snapshot of the emerging tomato genome sequence. *Plant Genome* 2: 78–92

- Nelson BK, Cai X, Nebenführ A (2007) A multicolored set of in vivo organelle markers for co-localization studies in Arabidopsis and other plants. *Plant J* **51**: 1126–1136
- Nunes-Nesi A, Sulpice R, Gibon Y, Fernie AR (2008) The enigmatic contribution of mitochondrial function in photosynthesis. *J Exp Bot* **59**: 1675–1684
- Oleski N, Mahdavi P, Bennett AB (1987) Transport properties of the tomato fruit tonoplast. II. Citrate transport. *Plant Physiol* **84**: 997–1000
- Regev-Rudzki N, Karniely S, Ben-Haim NN, Pines O (2005) Yeast aconitase in two locations and two metabolic pathways: seeing small amounts is believing. *Mol Biol Cell* **16**: 4163–4171
- Roessner U, Luedemann A, Brust D, Fiehn O, Linke T, Willmitzer L, Fernie AR (2001) Metabolic profiling allows comprehensive phenotyping of genetically or environmentally modified plant systems. *Plant Cell* **13**: 11–29
- Roessner-Tunali U, Hegemann B, Lytovchenko A, Carrari F, Bruedigam C, Granot D, Fernie AR (2003) Metabolic profiling of transgenic tomato plants overexpressing hexokinase reveals that the influence of hexose phosphorylation diminishes during fruit development. *Plant Physiol* **133**: 84–99
- Sadka A, Artzi B, Cohen L, Dahan E, Hasdai D, Tagari E, Erner Y (2000a) Arsenite reduces acid content in citrus fruit, inhibits activity of citrate synthase but induces its gene expression. *J Am Soc Hortic Sci* **125**: 288–293
- Sadka A, Dahan E, Cohen L, Marsh KB (2000b) Aconitase activity and expression during the development of lemon fruit. *Physiol Plant* **108**: 255–262
- Schauer N, Semel Y, Balbo I, Steinfath M, Repsilber D, Selbig J, Pleban T, Zamir D, Fernie AR (2008) Mode of inheritance of primary metabolic traits in tomato. *Plant Cell* **20**: 509–523
- Schauer N, Semel Y, Roessner U, Gur A, Balbo I, Carrari F, Pleban T, Perez-Melis A, Bruedigam C, Kopka J, et al (2006) Comprehensive metabolic profiling and phenotyping of interspecific introgression lines for tomato improvement. *Nat Biotechnol* **24**: 447–454
- Schuch W (1994) Improving tomato fruit quality and the European regulatory framework. *Euphytica* **79**: 287–291
- Shimada T, Nakano R, Shulaev V, Sadka A, Blumwald E (2006) Vacuolar citrate/H⁺ symporter of citrus juice cells. *Planta* **224**: 472–480
- Shiratake K, Martinoia E (2007) Transporters in fruit vacuoles. *Plant Biotechnol* **24**: 127–133
- Sienkiewicz-Porzucek A, Nunes-Nesi A, Sulpice R, Lisec J, Centeno DC, Carillo P, Leisse A, Urbanczyk-Wochniak E, Fernie AR (2008) Mild reductions in mitochondrial citrate synthase activity result in a compromised nitrate assimilation and reduced leaf pigmentation but have no effect on photosynthetic performance or growth. *Plant Physiol* **147**: 115–127
- Sienkiewicz-Porzucek A, Sulpice R, Osorio S, Krahnert I, Leisse A, Urbanczyk-Wochniak E, Hodges M, Fernie AR, Nunes-Nesi A (2010) Mild reductions in mitochondrial NAD-dependent isocitrate dehydrogenase activity result in altered nitrate assimilation and pigmentation but do not impact growth. *Mol Plant* **3**: 156–173
- Steinhauser MC, Steinhauser D, Gibon Y, Bolger M, Arrivault S, Usadel B, Zamir D, Fernie AR, Stitt M (2011) Identification of enzyme activity quantitative trait loci in a *Solanum lycopersicum* × *Solanum pennellii* introgression line population. *Plant Physiol* **157**: 998–1014
- Steinhauser MC, Steinhauser D, Koehl K, Carrari F, Gibon Y, Fernie AR, Stitt M (2010) Enzyme activity profiles during fruit development in tomato cultivars and *Solanum pennellii*. *Plant Physiol* **153**: 80–98
- Sulpice R, Trenkamp S, Steinfath M, Usadel B, Gibon Y, Witucka-Wall H, Pyl ET, Tschoep H, Steinhauser MC, Guenther M, et al (2010) Network analysis of enzyme activities and metabolite levels and their relationship to biomass in a large panel of *Arabidopsis* accessions. *Plant Cell* **22**: 2872–2893
- Sweetlove LJ, Beard KF, Nunes-Nesi A, Fernie AR, Ratcliffe RG (2010) Not just a circle: flux modes in the plant TCA cycle. *Trends Plant Sci* **15**: 462–470
- Tieman D, Bliss P, McIntyre LM, Blandon-Ubeda A, Bies D, Odabasi AZ, Rodríguez GR, van der Knaap E, Taylor MG, Goulet C, et al (2012) The chemical interactions underlying tomato flavor preferences. *Curr Biol* **22**: 1035–1039
- van der Merwe MJ, Osorio S, Araújo WL, Balbo I, Nunes-Nesi A, Maximova E, Carrari F, Bunik VI, Persson S, Fernie AR (2010) Tricarboxylic acid cycle activity regulates tomato root growth via effects on secondary cell wall production. *Plant Physiol* **153**: 611–621
- Williams TCR, Miguet L, Masakapalli SK, Kruger NJ, Sweetlove LJ, Ratcliffe RG (2008) Metabolic network fluxes in heterotrophic Arabidopsis cells: stability of the flux distribution under different oxygenation conditions. *Plant Physiol* **148**: 704–718